Inhibition of mitochondrial respiration by nitric oxide rapidly stimulates cytoprotective GLUT3-mediated glucose uptake through 5′-AMP-activated protein kinase

Pilar CIDAD*, Angeles ALMEIDA*† and Juan P. BOLAÑOS*‡[1]

*Departamento de Bioquímica y Biología Molecular, Universidad de Salamanca, Campus Miguel de Unamuno, 37007 Salamanca, Spain, †Unidad de Investigación, Hospital Universitario de Salamanca, Salamanca, Spain, and ‡Centro Nacional de Investigaciones Cardiovasculares (CNIC), Madrid, Spain

Recently, we have reported that the inhibition of mitochondrial respiration by nitric oxide (NO) leads to an up-regulation of glycolysis and affords cytoprotection against energy failure through the stimulation of AMPK (5′-AMP-activated protein kinase) [Almeida, Moncada and Bolaños (2004) Nat. Cell Biol. **6**, 45–51]. To determine whether glucose transport contributes specifically to this effect, we have now investigated the possible role of NO in modulating glucose uptake through GLUT3, a facilitative high-affinity glucose carrier that has been suggested to afford cytoprotection against hypoglycaemic episodes. To do so, GLUT3-lacking HEK-293T cells (human embryonic kidney 293T cells) were transformed to express a plasmid construction encoding green fluorescent protein-tagged GLUT3 cDNA. This carrier was preferentially localized to the plasma membrane, was seen to be functionally active and afforded cytoprotection against low glucose-induced apoptotic death. Inhibition of mitochondrial respiration by NO triggered a rapid, cGMP-independent enhancement of GLUT3-mediated glucose uptake through a mechanism that did not involve transporter translocation. Furthermore, the functional disruption of AMPK by the RNA interference strategy rendered cells unable to respond to NO by activating GLUT3-mediated glucose uptake. These results suggest that the inhibition of mitochondrial respiration by NO activates AMPK to stimulate glucose uptake, thereby representing a novel survival pathway during pathophysiological conditions involving transient reductions in the supply of cellular glucose.

Key words: 5′-AMP-activated protein kinase (AMP kinase), cytoprotection, glucose uptake, glycolysis, mitochondria, nitric oxide.

INTRODUCTION

GLUT3 is a member of facilitative glucose transporters found mainly in neuronal cells [1]. In view of the high apparent affinity of neurons for glucose [2], it has been postulated that the activity of this transporter would play a beneficial role during glucose deprivation or hypoxic episodes [3–6]. We have described previously that after injurious stimuli, such as hypoxia, glucose deprivation or LPS (lipopolysaccharide) treatment, astrocytes, which are cells predominantly expressing the GLUT1 transporter [7], respond by increasing GLUT3 mRNA and protein levels, as well as the rate of glucose uptake [8]. Since these cells do not express GLUT3 under normal conditions [7–9] and since they synthesize NO prominently on LPS treatment [10–14], we speculated that NO might be involved in the GLUT3-mediated glucose uptake process [8]. However, this issue was not addressed directly, and hence the mechanism and possible beneficial function of GLUT3 have remained elusive.

In skeletal-muscle cells, expressing mainly GLUT4 and to a lesser extent GLUT1 and GLUT3, NO stimulates glucose uptake in a cGMP-dependent fashion [15,16] by promoting GLUT4 translocation to the PM (plasma membrane) [17]. This effect can be triggered by AMPK (5′-AMP-activated protein kinase), a cell energy sensor that is activated in response to high AMP/ATP ratios [18] and that phosphorylates metabolic substrates to maintain the energy balance [19]. eNOS (endothelial nitric oxide synthase) is an AMPK substrate during the cell energy loss associated with ischaemia in the rat heart [20]. In fact, the activation of AMPK by the AMP analogue 5-aminoimidazole-4-carboxamide ribonucleoside triggers eNOS-mediated NO production, which is responsible for the cGMP-dependent increase in glucose uptake observed in skeletal-muscle cells [17]. However, such a signalling cascade has not been observed during the AMPK-triggered increase in glucose uptake that occurs in cells mainly expressing GLUT1, but not GLUT4, GLUT2 or GLUT3, such as rat liver epithelial clone 9 cells [21], 3T3-L1 preadipocytes or myoblasts [22]. Thus the stimulation of GLUT1 by AMPK in these cells does not involve translocation, but instead activation of the transporter at the PM [22,23]. Furthermore, the underlying mechanism is NO- and cGMP-independent [23]. Accordingly, the mechanism by which NO and AMPK stimulate glucose uptake appears to be a function of the major glucose carrier expressed in the cell.

Recently, we have found that NO switches on glycolysis in astrocytes and in HEK-293T cells (human embryonic kidney 293T cells) through a mechanism involving AMPK [24]. Since NO inhibits cytochrome *c* oxidase [25] and decreases ATP concentrations [26], we conjectured that the NO-mediated inhibition of mitochondrial respiration might trigger, through AMPK, a defensive signalling cascade focused on the utilization and metabolism of glucose [24]. Prompted by this notion and by previous findings indicating that GLUT3 may play a neuroprotective role [3–6,27], the aim of the present study was to investigate whether NO modulates GLUT3-mediated glucose uptake, addressing the mechanism underlying this phenomenon.

Abbreviations used: 7-AAD, 7-amino-actinomycin D; AMPK, 5′-AMP-activated protein kinase; APC, allophycocyanin; DETA-NO, (Z)-1-[2-aminoethyl-*N*-(2-ammonioethyl)amino] diazen-1-ium-1,2-diolate; DMEM, Dulbecco's modified Eagle's medium; eNOS, endothelial nitric oxide synthase; GFP, green fluorescent protein; HEK-293T cells, human embryonic kidney-293T cells; LDM, low-density intracellular membrane; LPS, lipopolysaccharide; ODQ, 1H-(1,2,4)oxadiazolo[4,3-α]quinoxalin-1-one; PM, plasma membrane; RT, reverse transcriptase; siRNA, small interfering RNA.

[1] To whom correspondence should be addressed (email jbolanos@usal.es).

EXPERIMENTAL

RT (reverse transcriptase)–PCR analysis

Total RNA was purified from HEK-293T cells using a commercially available kit (Sigma, Madrid, Spain). GLUT1, GLUT3 and GLUT4 expression was analysed by 2 % agarose electrophoresis in DNA-free RNA aliquots (1 μg) after RT–PCR (50 min at 48 °C for reverse transcription; 35 cycles of 30 s at 95 °C, 1 min at 58, 53.1 or 59.1 °C for GLUT1, GLUT3 and GLUT4 respectively and 30 s at 72 °C; 10 min at 72 °C) using the following forward and reverse oligonucleotides respectively: 5′-GGACAGCTGACGTGACCCATG-3′ and 5′-TGGAACAGCTCCTCGGGTGTC-3′ for GLUT1 (accession no. NM_006516; nt 877–1630); 5′-TCCTGCTCTCCTACAAAGTGC-3′ and 5′-GTCCTTTCCAGATCTATCTGC-3′ for GLUT3 (accession no. NM_006931; nt 821–1676); 5′-CCTGACAGGCTGGGCCGATGT-3′ and 5′-CCTGGCCCCTCAGTCGTTCTC-3′ for GLUT4 (accession no. NM_001042; nt 883–1684). In no case was a band detected by PCR without reverse transcription.

GLUT3 and GLUT1 plasmid constructions

Rat GLUT3 cDNA was obtained by RT–PCR of total RNA isolated from LPS (1 μg/ml, 18 h)-treated rat astrocytes as template with the following sense and antisense primers respectively: 5′-CCGGAATTCCGGAGCTAGGTTGGGACC-3′ and 5′-CCGGAATTCCACAGTGGAGGGA-3′. The cDNA product was purified, digested and subcloned into the *Eco*RI site of Bluescript II KS$^+$ (pBS-rG3). GLUT3 cDNA was then amplified from pBS-rG3 as template, using the following sense and antisense primers respectively: 5′-CCGGAATTCCGGAGCTAGGTTGGGACC-3′ and 5′-CCGGAATTCGGGCATTGCCAGGGGTCTCC-3′ (six codons coding for amino acids 488–493, double underline; stop codon excluded). Full-length rat GLUT1 cDNA was amplified from pBS-rG1 (Bluescript II KS$^-$; generously provided by Professor A. Zorzano, University of Barcelona, Spain) as template using the following sense and antisense primers respectively: 5′-CCGGAATTCACAGCCCGCACAGCTTGAGCCTC-3′ and 5′-CCGGAATTCCCACTTGGGAGTCAGCCCCCAGAGGGTG-3′ (*Eco*RI site, single underline; nine codons encoding for amino acids 484–492, double underline; stop codon excluded). GLUT3 and GLUT1 PCR products were subcloned into the *Eco*RI site of the pd2EGFP-N1 mammalian expression vector (henceforth named pEGFP; ClonTech Laboratories, Palo Alto, CA, U.S.A.). The resulting plasmid constructions (pEGFP.G3 or pEGFP.G1) encode the full-length GLUT3 or GLUT1 fused at their C-termini to GFP (green fluorescent protein). Full-length GLUT3 or GLUT1 cDNAs, digested from pBS-rG3, were also subcloned into the *Eco*RI site of the pcDNA3 mammalian expression vector (Invitrogen, Madrid, Spain; pcDNA3-G3). All oligonucleotides were purchased from Isogen Life Technologies (Maarsen, The Netherlands), and the plasmid constructions were confirmed by DNA sequencing.

Design of AMPK siRNA (small interfering RNA)

AMPK-α_1 catalytic subunit disruption was achieved by RNA interference using a vector-based small hairpin RNA approach [28]. The target sequence was 5′-GAATCCTGTGACAAGCACA-3′ (nt 1332–1350, accession no. NM_006251) and was BLAST-confirmed for specificity. Forward and reverse synthetic 64 nt oligonucleotides (Isogen Life Technologies) were designed, annealed and inserted into the *Bgl*II–*Hin*dIII sites of pSuper mammalian expression vector (Oligoengine, Seattle, WA, U.S.A.) according to the manufacturer's instructions. These constructions express a 19-bp, 9-nt stem-loop RNA structure (small hairpin RNA) specifically targeted against AMPK-α_1 mRNA, and we have confirmed the effectiveness and specificity of the siRNAi previously [24]. To eliminate the potential unwanted interference of the siRNAs [29], all control cells were transfected with firefly luciferase-targeted siRNA-expressing pSuper vector (sequence 5′-CTGACGCGGAATACTTCGA-3′) as described in [30].

Cell transfections

HEK-293T cells were used for the experiments, and were incubated in DMEM (Dulbecco's modified Eagle's medium) containing 10 % (v/v) fetal calf serum (Roche Diagnostics). Cells were seeded 24 h before the experiments at 10^5 cells/cm^2. To express the GFP-carrying GLUT3 or GLUT1 transporters, transfections of HEK-293T cells with pEGFP.G3 or pEGFP.G1 were performed using LIPOFECTAMINE™ 2000 (Invitrogen) for 24 h, according to the manufacturer's instructions. As controls, cells were transfected with equivalent amounts of DNA of the basic plasmid vector pEGFP. Full-length GLUT3 or GLUT1 cDNA-carrying pcDNA3 plasmid vector (pcDNA3-G3 or pcDNA-G1) was also expressed for experiments focused to ensure that the GFP domains of GLUT3-GFP or GLUT1-GFP did not interfere in the glucose uptake process. To disrupt AMPK activity, the cells were transfected for 62 h (LIPOFECTAMINE™ 2000) with AMPK-targeted pSuper (AMPK siRNA), using cells transfected with luciferase-targeted pSuper as controls. The efficiencies of transfections were approx. 95 %, as assessed by quantification of fluorescent cells. The subcellular localizations of the plasmid constructions expressed were visualized under a Leica fluorescence microscope (Leica Microsystems Wetzlar, Wetzlar, Germany), using the I3-blue GFP filter (450–490 nm excitation wavelength) at 100× magnification, and microphotographs were taken using a Leica IM-50 digital camera. Functional expression of GLUT3 or GLUT1 cDNA-encoding vectors was confirmed by 2-deoxy-D-[U-^{14}C]glucose uptake and the efficacy of the AMPK siRNA procedure was checked by Western blotting.

Incubations of cells with NO

To expose the cells to controlled amounts of NO, cells were incubated in DMEM containing DETA-NO {(Z)-1-[2-aminoethyl-*N*-(2-ammonioethyl)amino] diazen-1-ium-1,2-diolate; Alexis Corporation, San Diego, CA, U.S.A.} at 0.5 mM, i.e. the concentration seen to release continuously approx. 1.4 μM of NO for approx. 18 h at 37 °C, as measured by a NO-sensitive electrode (World Precision Instruments, Sarasota, FL, U.S.A.; results not shown). To ensure immediate exposure of the cells to NO, all DETA-NO-containing solutions were always preincubated in DMEM at 37 °C for 20 min before addition to the cells. Controls (NO-untreated cells) were performed using a degraded (37 °C for 48 h) DETA-NO solution. To block guanylate cyclase activity, cells were incubated with ODQ {1H-(1,2,4)oxadiazolo[4,3-α]quinoxalin-1-one; 10 μM; Alexis Corporation} as from 5 min before DETA-NO incubations. To activate guanylate cyclase activity, cells were incubated with BAY41-2272 [31] (2 μM; generously provided by Professor S. Moncada, Wolfson Institute for Biomedical Research, London, U.K.) for 1 h. The changes in cGMP concentrations were confirmed in the cells untreated or treated with DETA-NO, ODQ or BAY41-2272 in the presence of the phosphodiesterase inhibitor isobutylmethylxanthine (1 mM) using a [^{3}H]cGMP radioimmunoassay (Amersham Biosciences, Bucks., U.K.), according to the manufacturer's instructions.

Oxygen consumption, ATP and AMP measurements

A Clark-type electrode (Rank Brothers, Cambridge, U.K.) was used to estimate the rate of O_2 consumption in cells incubated with

DETA-NO (0.5 mM) for 1 h. Since NO-mediated inhibition of oxygen consumption has been shown to depend strongly on the O_2 concentration [32], the rate of oxygen consumption was assessed at an initial O_2 concentration of approx. 200 μM (saturation) for 15 min; after this period, the final O_2 concentration was approx. 175 μM. The rate of O_2 consumption was calculated from the slopes and expressed as nmol of O_2 consumed $\cdot$ min^{-1} $\cdot$ $(1 \times 10^6$ cells$)^{-1}$. Mitochondrial respiration was estimated by subtracting the rates of O_2 consumption obtained in control and DETA-NO-treated cells from that obtained with oligomycin (5 μM)-treated cells. ATP concentrations were measured by chemiluminescence in $KHCO_3$-neutralized $HClO_4$ cell extracts using a commercially available kit (Sigma) and according to the manufacturer's instructions. AMP concentrations were determined by an enzymic method [33] in $KHCO_3$-neutralized $HClO_4$ cell extracts, using 15×10^6 cells per determination.

Glucose uptake measurements

Cells were washed with PBS (pH 7.4) and preincubated in DMEM for 2 h. For uptake experiments, cells were further incubated at 37 °C in glucose-free DMEM (Sigma) containing increasing concentrations of D-glucose (25–250 μM) in the presence of 0.1 μCi/ml 2-deoxy-D-[U-^{14}C]glucose (Amersham Biosciences). After 5 min (except for the time-course experiments), the medium was removed and cells were rapidly washed three times with ice-cold PBS containing 50 mM glucose. Cells were then lysed with 10 mM NaOH/0.1 % (v/v) Triton X-100 and the radioactive lysates were used for liquid scintillation (Universol; ICN Biomedicals, Irvine, CA, U.S.A.) counting (98 % efficiency; LS 6500; Beckman Instruments, Palo Alto, CA, U.S.A.) and protein concentration determinations [34], using BSA as standard. Blanks in which the radioactive medium had been removed as quickly as possible (< 1 s) were performed in parallel, and their radioactivity was subtracted from the sample values. Preliminary experiments (results not shown) confirmed that the rate of 2-deoxy-D-[U-^{14}C]-glucose uptake was linear with time (1–10 min range). In all uptake experiments, the maximum glucose concentration used was 250 μM to prevent the possible limitation of the uptake process by glucose phosphorylation by hexokinase [2]; unless otherwise specified, 2-deoxyglucose uptake experiments were performed using 250 μM glucose.

Membrane fractionation

To separate plasma and intracellular membranes, we used a previously reported method [35] with some modifications. Cells incubated on 60 cm^2 plates were washed with PBS, scraped off with ice-cold homogenization buffer [0.25 M sucrose, 2 mM EGTA, 20 mM Hepes plus the protease inhibitor cocktail (100 μM *N*-α-p-tosyl-L-lysine chloromethane ketone, 100 μM PMSF, 1 mM phenanthroline, 10 μg/ml pepstatin A, 100 μM *N*-tosyl-L-phenylalanine chloromethane ketone, 10 μg/ml leupeptin, 10 μg/ml aprotinin, 10 μg/ml soya bean trypsin inhibitor), pH 4], and homogenized in a glass–glass homogenizer (15 strokes). Homogenates were centrifuged at 800 ***g*** for 5 min at 4 °C. The supernatant was collected and kept on ice, and the pellet was resuspended in 1 ml of homogenization buffer, homogenized and centrifuged as above. Both supernatants were pooled and centrifuged at 24 000 ***g*** for 1 h at 4 °C. The pellet was lysed in 100 μl of RIPA [12.5 mM Na_2HPO, 1 % Triton X-100, 0.1 % (w/v) SDS, 2 mM EDTA, 150 mM NaCl and the protease inhibitors cocktail, pH 7.2], and was considered the partially purified PM fraction. The supernatant was centrifuged at 190 000 ***g*** for 1 h at 4 °C (Optima™ XL-100K Ultracentrifuge; Beckman Instruments) and the resulting pellet was lysed in 50 μl of RIPA, and was considered the LDM (low-density intracellular membrane) fraction. Both the PM and LDM fractions were resolved by SDS/PAGE and subjected to anti-GFP Western blotting.

Digestion of glycoproteins with N-glycosidase F

Both PM and LDM fractions were resuspended in 12.5 mM Na_2HPO_4, 1 % Triton X-100, 0.1 % SDS, 2 mM EDTA, 150 mM NaCl, 1 % (w/v) 2-mercaptoethanol, protease inhibitor cocktail, and incubated with 0.7 unit of N-glycosidase F (Roche Diagnostics) at 37 °C for 18 h with shaking. The digested samples were resolved by SDS/PAGE and subjected to anti-GFP Western blotting.

Northern blotting

Purified (Sigma) total RNA samples were electrophoresed (15 μg of RNA/line) on a 1 % (w/v) agarose-formaldehyde gel. After transfer to a GeneScreen Plus membrane (NEN Life Science Products, Boston, MA, U.S.A.) and cross-linking with UV irradiation (UV Stratalinker, Mod. 2400; Genetic Research Instruments, Essex, U.K.), membranes were hybridized for 18 h at 65 °C in the presence of the appropriate random-primed [α-^{32}P]dCTP-radiolabelled (Amersham Biosciences) cDNA probe and exposed to Kodak XAR-5 film. As cDNA probe, a 0.9 kb fragment (corresponding to the 3′-UTR region, nt 1649–2571, accession no. NM_13979) of rat GLUT1, obtained from *Sac*I and *Eco*RI-digestion of pBS-rG1 vector, and a 0.6 kb fragment (nt 698–1260, accession no. X61093) of mouse GLUT3 (generously provided by Professor A. Zorzano) were used.

Western blotting

Cells were scraped off the plastic with lysis buffer (12.5 mM Na_2HPO_4, 116 mM NaCl, 0.5 M EDTA, 1 % Triton X-100, 0.1 % SDS and the protease inhibitor cocktail, pH 7), and 10, 20 or 50 μg of protein from PM, LDM or whole-cell extracts respectively (extemporarily determined by the method of Bradford [36] using ovalbumin as standard) and the BenchMark™ prestained protein ladder (Isogen Life Technologies) were electrophoresed on 10 % acrylamide gel (MiniProtean®; Bio-Rad Laboratories) and transferred to a Hybond® nitrocellulose membrane (Amersham Biosciences). Membranes were blocked with 10 % (w/v) low-fat milk in 20 mM Tris, 500 mM NaCl, 0.1 % (w/v) Tween 20 (pH 7.5) for 1 h, and incubated in the presence of either anti-GFP (provided by Professor S. Moreno, Centro de Investigación del Cancer, Salamanca, Spain), anti-Na^+-K^+-ATPase-α_1 subunit (Santa Cruz Biotechnology, Santa Cruz, CA, U.S.A.), anti-AMPK-α_1 and anti-phospho-AMPK-α_1-Thr-172 (Cell Signalling Technology, Beverly, MA, U.S.A.) or anti-6-phosphofructo-1-kinase, muscle isoform (generously provided by Dr E. Fernández, University of Salamanca, Spain) at 4 °C overnight. Horseradish peroxidase anti-rabbit IgG-treated membranes (Santa Cruz Biotechnology) were immediately developed by luminol-chemiluminescence. Films were scanned and the intensity of the bands was quantified using an image analyser system (NIH Image), kindly supplied by Wayne Rasband (National Institutes of Health, Bethesda, MD, U.S.A.).

Flow cytometric analysis of apoptosis

APC (allophycocyanin)-conjugated annexin-V and 7-AAD (7-amino-actinomycin D) (Becton-Dickinson Biosciences, Erembodegen, Belgium) were used to determine quantitatively the percentage of apoptotic cells by flow cytometry. After experimental

treatments, cells were carefully scraped off and stained with annexin V-APC and 7-AAD, according to the manufacturer's instructions. After 15 min, GFP, annexin V-APC and 7-AAD signals were analysed on the FL1, FL4 and FL3 channels respectively using a FACScalibur flow cytometer (15 mW argon ion laser tuned at 488 nm; CellQuest software, Becton-Dickinson Biosciences). Among GFP^+ cells, those annexin $V\text{-}APC^+$ cells that were $7\text{-}AAD^-$ were considered to be apoptotic.

Statistical analyses

Results are expressed as the means $\pm$ S.E.M. values for at least three independent experiments. Statistical significance was evaluated by one-way analysis followed by the least significant difference multiple range test.

RESULTS

Functional expression of GFP-tagged GLUT3 protects cells against low-glucose-induced apoptotic death

In view of the possible association between NO production and GLUT3 activity in astrocytes [8], we first decided to investigate the regulation of glucose uptake activity in cells overexpressing GLUT3 transporter. To do so, first, a plasmid vector encoding GLUT3 fused at its C-terminus with GFP (pEGFP.G3) was constructed. RT–PCR analyses of HEK-293T cells revealed that GLUT3, as GLUT4, was only negligibly expressed; however, the expression of GLUT1 was found to be prominent (Figure 1a). To express pEGFP.G3 plasmid construction, these HEK-293T cells were used because (i) as astrocytes [7–9] these cells express traces of GLUT3 (Figure 1a), and (ii) they show high transfection efficiencies and are thus more suitable for studying glucose transporter-mediated 2-deoxyglucose uptake. In view of the observation that GLUT1 was prominently expressed (Figure 1a), we also studied the possible regulation of this transporter by NO, and a plasmid vector encoding GLUT1 at its C-terminus with GFP (pEGFP.G1) was also constructed. As shown in Figure 1(b), Northern-blot analyses confirmed very low endogenous GLUT3 mRNA (4.0 kb) and prominent GLUT1 mRNA (2.9 kb) expression. To confirm that the pEGFP.G3 and pEGFP.G1 expression plasmids had been transcribed, the corresponding mRNA levels in the transfected HEK-293T cells were analysed. As depicted in Figure 1(b), the 2.9 kb transcripts from pEGFP.G3 and pEGFP.G1 were prominently expressed, in comparison with the signal obtained at 2.9 kb in cells transfected with the empty vector (pEGFP). To test whether the translational product of the mRNAs had the predicted size, the expressions of these constructions were then analysed by Western blotting using an anti-GFP antibody. As shown in Figure 1(c), transfection with pEGFP only yielded the expected 31 kDa protein corresponding to GFP, whereas transfection with pEGFP.G3 and pEGFP.G1 only expressed the expected 85 kDa bands corresponding to the GLUT3– and GLUT1–GFP fusion proteins. To elucidate the subcellular localization of the chimaeras, the PM and LDM fractions, untreated or treated with N-glycosidase-F, of transfected cells were subjected to Western blotting. As shown in Figure 1(d), the PM fraction was highly enriched in PM as revealed by Na^+-K^+-ATPase immunoblotting, whereas the LDM fractions contained very little or undetectable Na^+-K^+-ATPase. Both fractions showed the typical band smears corresponding to the glycosidated and non-glycosidated pEGFP.G3 and pEGFP.G1 expression products, as assessed with anti-GFP (Figure 1d). In fact, treatment with N-glycosidase-F transformed most of the higher-molecular mass bands into the lower-molecular mass bands, which had the expected 85 kDa chimaera sizes. Although these Western-blotting results suggest localization of the fusion proteins at the PM, we further studied the localization of the transporters in the intact, transfected HEK-293T cells by fluorescence microscopy using a GFP filter. As depicted in Figure 1(d) (lower panel), cells transfected with the empty vector (pEGFP) showed the typical diffuse fluorescence distribution due to soluble GFP protein, whereas the observation of the fluorescence of cells transfected with pEGFP.G3 and pEGFP.G1 confirmed that these transporters were localized at the PM. However, most GLUT3–GFP was present at the PM, but GLUT1–GFP was also located intracellularly (Figure 1d, lower panel).

Next, we investigated whether the expressed transporters were functional. For this purpose, the rate of 2-deoxyglucose uptake was measured in pEGFP, pEGFP.G3, pEGFP.G1, pcDNA3, pcDNA3-G3 (lacking GFP cDNA) or pcDNA3-G1 (lacking GFP cDNA)-transfected cells using 2-deoxy-D-[U-^{14}C]glucose and low glucose concentrations (25–250 μM) for 5 min. As shown in Figure 1(e), the rates of 2-deoxyglucose uptake in pEGFP.G3- and pEGFP.G1-transfected cells were higher when compared with pEGFP-transfected cells, at least in the 25–250 μM range of extracellular glucose concentrations. In view that GLUT1 is the main endogenous transporter expressed in these cells (Figure 1a), we assume that 2-deoxyglucose uptake in control (pEGFP-transfected) cells (Figure 1e) would be mainly due to this transporter. Furthermore, 2-deoxyglucose uptake in pEGFP.G3-transfected cells was higher than that observed in pEGFP.G1-transfected cells (Figure 1e). In addition, the increases in 2-deoxyglucose uptake obtained by transfection of cells with pEGFP.G3 or pEGFP.G1 when compared with the empty vector (pEGFP) were very similar to the enhancements observed by transfection with pcDNA3-G3 or pcDNA3-G1 when compared with the corresponding empty vector pcDNA3 (Figure 1f). These results strongly suggest that the expressed GLUT3–GFP and GLUT1–GFP chimaeras are functional, and that the GFP domains of the fusion proteins do not interfere with the glucose uptake process.

In light of previous results suggesting that GLUT3 might be neuroprotective [3–6], we next investigated whether the expression of this, and GLUT1 transporters protected cells against apoptosis induced by glucose deprivation. For this purpose, pEGFP-transfected HEK-293T cells were first incubated in the presence of different concentrations of glucose for 64 h, and the proportion of apoptotic cells was analysed at different time points by flow cytometry using annexin V and 7-AAD staining. As shown in Figure 1(g), cells incubated in DMEM containing 5.5 mM glucose were resistant up to 48 h of incubation, whereas glucose deprivation resulted in a time- and concentration-dependent increase in the number of apoptotic cells. In view of these results, the vulnerability of pEGFP-, pEGFP.G3- and pEGFP.G1-transfected cells to glucose deprivation at 48 h of incubation was investigated. As depicted in Figure 1(h), transfection with pEGFP.G3 increased the resistance of HEK-293T cells to low glucose-induced apoptosis when compared with cells transfected with either pEGFP.G1 or pEGFP. Moreover, cells transfected with pEGFP.G3 showed higher resistance when compared with cells transfected with pEGFP.G1 against glucose deprivation (Figure 1h), suggesting that, although both expressed transporters are functional, GLUT3 transporter activity affords better protection than GLUT1.

NO increases GLUT3-mediated glucose uptake in a cGMP-independent fashion without altering transporter translocation

In view of the evidence that NO had increased glucose uptake in LPS-treated astrocytes [8] and, in light of previous results [15–17] suggesting that, at least GLUT4-mediated glucose uptake would be modulated by NO, we next decided to investigate whether NO

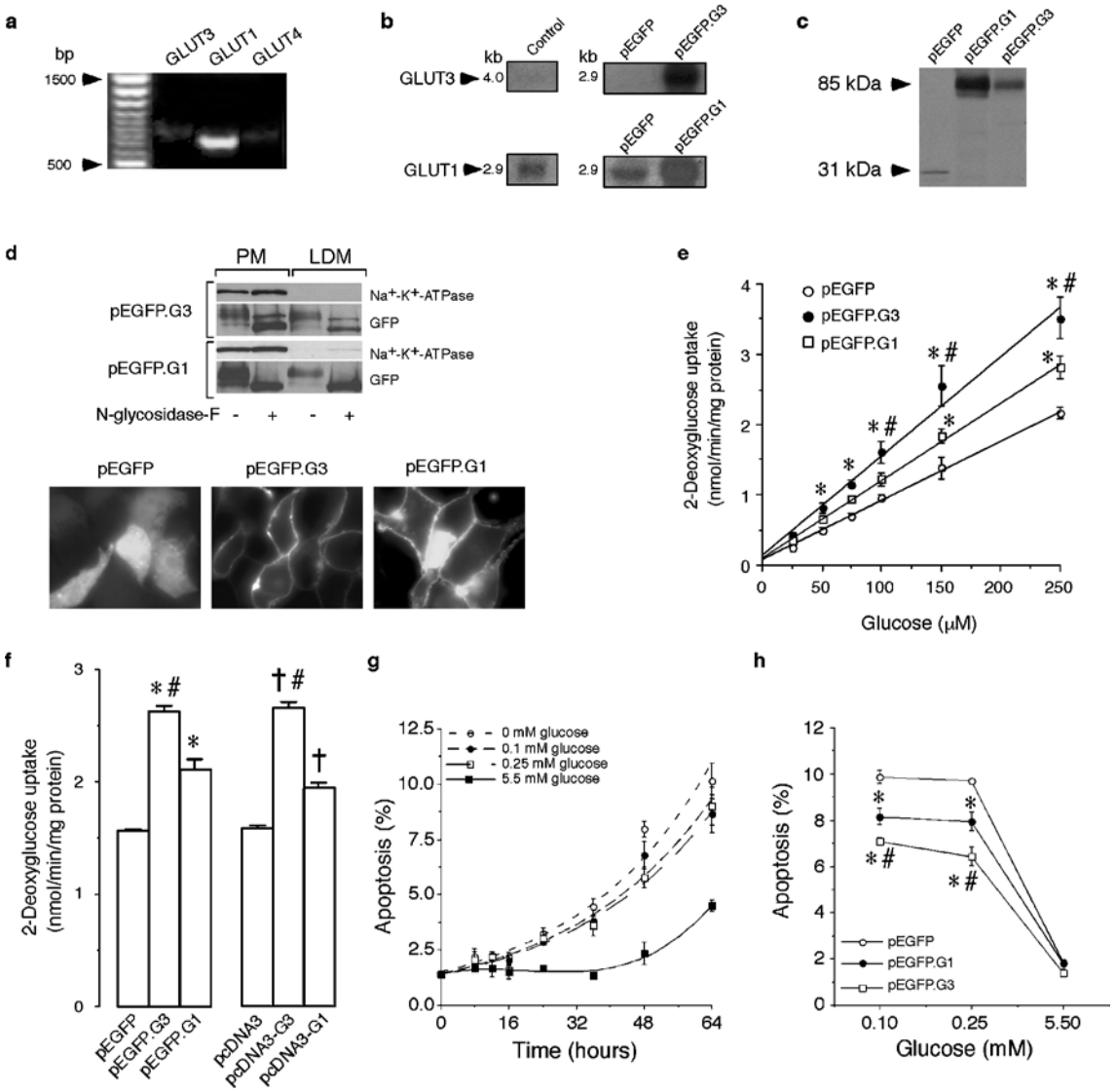

Figure 1 Functional expression of GFP-tagged GLUT3 protects cells against low-glucose-induced apoptotic death

(**a**) RT–PCR analyses of HEK-293T cells reveal high expression of GLUT1 glucose transporter and low/negligible GLUT3 or GLUT4 transporters (754, 856 and 802 bp cDNA fragments respectively). (**b**) Northern-blot analyses of HEK-293T cells confirm high GLUT1 mRNA and low GLUT3 mRNA expression. Transfection of these cells with the plasmid constructions encoding GLUT3-GFP or GLUT1-GPF (pEGFP.G3 or pEGFP.G1) fusion proteins confirms the expression of the corresponding transcripts, at the expected size, when compared with the cells transfected with the vector alone (pEGFP). (**c**) Western-blot analyses (anti-GFP) of transfected HEK-293T cells show the translational products of the plasmid vectors (pEGFP, pEGFP.G3 and pEGFP.G1) at the expected size. (**d**) Western-blot analysis of untreated or N-glycosidase-F-treated extracts obtained from cells expressing pEGFPG3 or pEGFP.G1 reveals localization of N-glycosylated GLUT3 and GLUT1 proteins at the PM. The fluorescence images of HEK-293T cells transfected with pEGFP reveal a diffused localization of GFP, PM localization of GLUT3-GFP (pEGFP.G3) and both cytosolic and PM localization of GLUT1-GFP (pEGFP.G1). (**e**) Expression of pEGFP.G3 afforded HEK-293T cells with higher rate of 2-deoxyglucose uptake than cells transfected with either pEGFP.G1 or pEGFP. (**f**) HEK-293T cells transfected with pEGFP.G3 or pEGFP.G1 took up 2-deoxyglucose (at 150 μM glucose) at a rate that was similar to those observed with pcDNA3-G3 or pcDNA3-G1, when compared with cells transfected with equivalent amounts of their respective empty vectors (pEFGFP or pcDNA3 respectively). (**g**) Glucose deprivation increased the proportion of apoptotic cells in a time- and concentration-dependent fashion (as assessed by annexin V^+/7-AAD^- by flow cytometry). (**h**) Overexpression of GLUT3 (pEGFP.G3) or GLUT1 (pEGFP.G1) in HEK-293T cells significantly reduced the apoptotic death caused by glucose deprivation when compared with the cells transfected with the empty vector (pEGFP). $^*P < 0.05$ versus pEGFP, $^\#P < 0.05$ versus pEGFP.G1 or pcDNA3-G1, †$P < 0.05$ versus pcDNA3.

might modulate GLUT3- and GLUT1-mediated glucose uptake using the plasmid constructions characterized herein. First, we assessed the effect of NO (1.4 μM for 1 h) on the rate of 2-deoxyglucose uptake (at 250 μM glucose) in cells transfected with pEGFP, pEGFP.G3 or pEGFP.G1. 2-Deoxyglucose uptake (at 250 μM glucose) rate values in control (NO-untreated)-transfected cells are shown in Figure 1(e), therefore we next expressed the data as the fraction values of 2-deoxyglucose uptake that were stimulated by NO (i.e. the difference between values obtained in NO-treated minus NO-untreated cells). As shown in Figure 2(a), NO-stimulated glucose uptake by $\sim$0.2 or $\sim$0.4 nmol $\cdot$ $min^{-1} \cdot$ (mg of protein)$^{-1}$ in cells transfected with pEGFP or pEGFP.G1 respectively, whereas GLUT3-transfected cells had an approx. 4-fold increase in NO-stimulated glucose uptake [by $\sim$0.8 nmol $\cdot$ $min^{-1} \cdot$ (mg of protein)$^{-1}$]. These results indicate that GLUT3-mediated glucose uptake is more sensitive than GLUT1 to stimulation by NO. Since Fryer et al. [17] had previously shown that NO-stimulated glucose uptake in skeletal-muscle cells is mediated by GLUT4 translocation to the PM, we investigated whether such a mechanism occurred in GLUT3- and

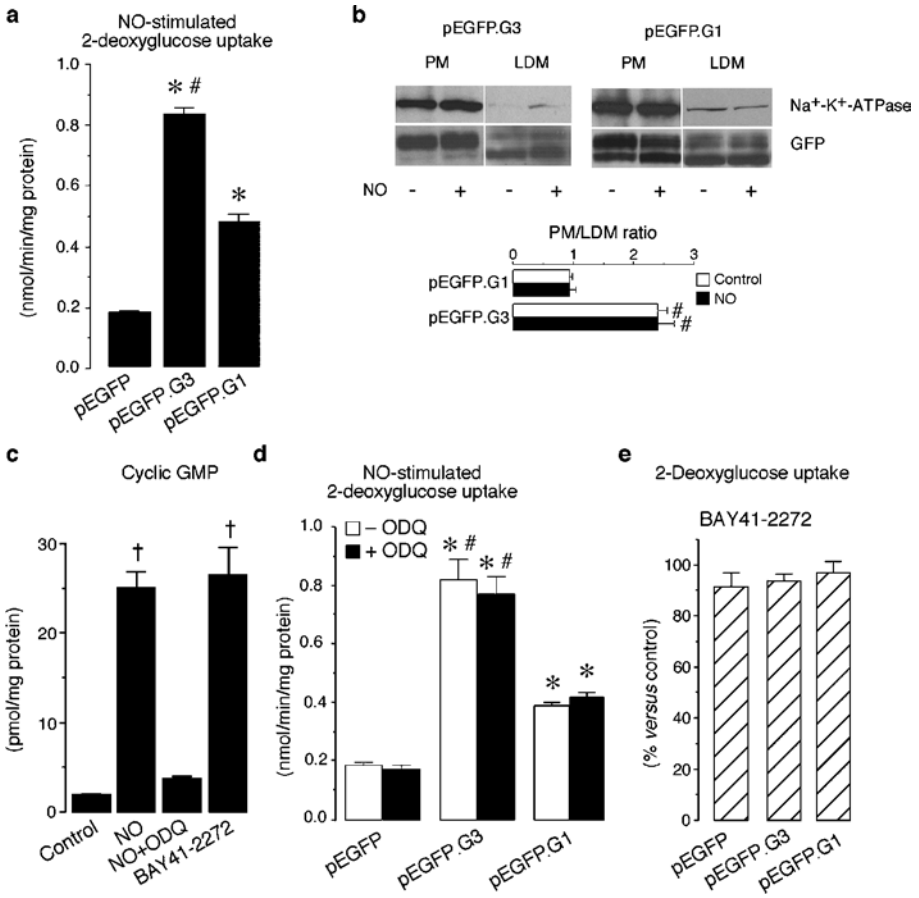

Figure 2 NO stimulates GLUT3-mediated glucose uptake in a cGMP-independent fashion without altering transporter translocation

(**a**) Incubation of GLUT3- and GLUT1-overexpressing (pEGFP.G3 and pEGFP.G1) HEK-293T cells with NO (1.4 μM, released from 0.5 mM DETA-NO for 1 h) elicited an approx. 4-fold (GLUT3) or approx. 2-fold (GLUT1) stimulation in the rate of glucose uptake when compared with pEGFP-transfected NO-treated cells. (**b**) Western-blot analysis of the bands of untreated or NO-treated cells overexpressing GLUT3 or GLUT1 revealed that NO did not alter the subcellular localization of the transporters between PM and LDM fractions. (**c**) NO triggered an increase in cGMP concentrations in HEK-293T cells that was prevented by ODQ (10 μM). BAY41-2272 (2 μM) increased cGMP concentrations. (**d**) ODQ did not prevent NO-activated 2-deoxyglucose uptake in GLUT3-overexpressing cells. (**e**) BAY41-2272 was unable to increase 2-deoxyglucose uptake in GLUT3- or GLUT1-overexpressing cells. $^{*}P < 0.05$ versus pEGFP, $^{\#}P < 0.05$ versus pEGFP.G1, $\dagger P < 0.05$ versus control.

GLUT1-transfected cells. As depicted in Figure 2(b), the relative abundances of GLUT3 or GLUT1 transporters between the PM and LDM fractions were unaltered by treatment with NO, strongly suggesting that the mechanism through which NO activates GLUT3- and GLUT1-mediated glucose uptake was independent of protein translocation. Since soluble guanylate cyclase is a key target of NO, and in light of previous data reporting that GLUT4 translocation in response to NO is mediated by cGMP [17], we wondered whether GLUT3- or GLUT1-mediated stimulation of glucose uptake might be a consequence of NO-triggered cGMP elevations. To address this issue, GLUT3- and GLUT1-transfected cells were incubated in the presence of NO, with or without the guanylate cyclase-specific inhibitor ODQ. The cells were also incubated with a potent and selective guanylate cyclase activator BAY41-2272 [31]. As shown in Figure 2(c), ODQ fully prevented the increase in cGMP concentrations triggered by NO, and BAY41-2272 strongly increased cGMP concentrations in NO-untreated cells. Noticeably, ODQ was unable to prevent NO-stimulated glucose uptake (Figure 2d), and BAY41-2272 did not increase glucose uptake in GLUT3- or GLUT1-transfected cells (Figure 2e). These results strongly suggest that cGMP is not involved in NO-stimulated GLUT3- or GLUT1-mediated glucose uptake.

Inhibition of mitochondrial respiration by NO increases GLUT3-mediated glucose uptake through AMPK

Having ruled out cGMP and GLUT3 or GLUT1 translocation as possible mechanisms for NO-activated glucose uptake, we next focused on the putative role of mitochondrial modulation by NO in the effect. Since NO is a well-known inhibitor of cytochrome *c* oxidase [25,32,37,38], we investigated whether NO inhibited mitochondrial respiration in HEK-293T cells. Incubation with 1.4 μM NO strongly inhibited mitochondrial respiration (Figure 3a), leading the cells to show a moderate decrease in ATP concentrations and a considerable increase in AMP concentration (Figure 3b). Since these parameters indicating an approx. 5-fold increase in the AMP/ATP ratio by NO are compatible with those described previously reporting the activation of the cell-energy sensor AMPK in exercise [19], the potential involvement of AMPK was then assessed. As shown in Figure 3(c), the treatment of these cells with NO for 1 h triggered AMPK-Thr-172 phosphorylation, confirming our recent findings pointing to the involvement of AMPK in glycolytic activation in astrocytes and HEK-293T in response to NO [24]. Next, the RNA interference strategy was implemented to inhibit AMPK. This was performed by transfecting HEK-293T with the pSuper expression

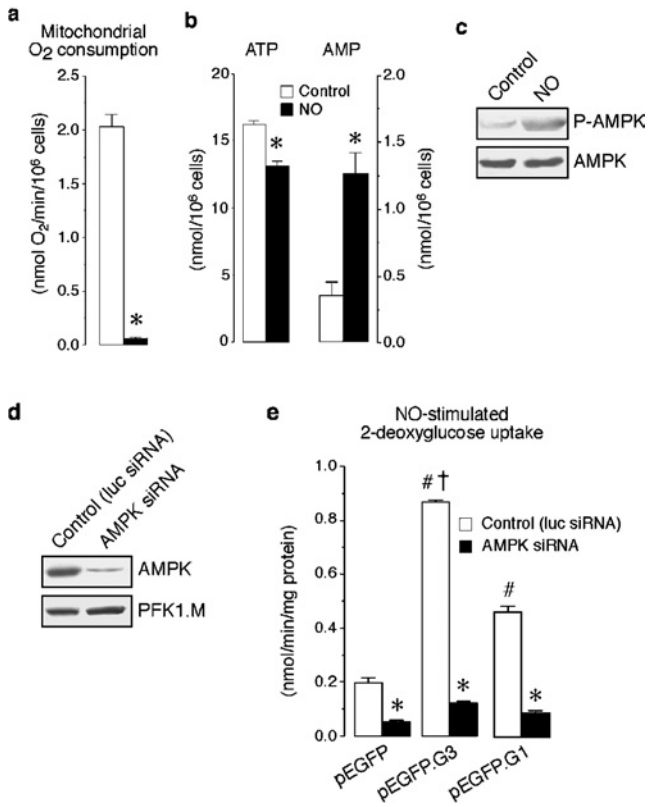

Figure 3 Inhibition of mitochondrial respiration by NO increases GLUT3-mediated glucose uptake through AMPK

(**a**) Incubation of HEK-293T cells with NO (1.4 μM for 1 h) strongly inhibited mitochondrial respiration, and (**b**) decreased ATP and increased AMP concentrations. (**c**) Western-blot analysis of NO-treated cells shows increased phosphorylation of AMPK-α_1-Thr-172 (P-AMPK). (**d**) Transfection of HEK-293T cells for 48 h with a pSuper vector encoding the AMPK siRNA markedly decreased AMPK levels when compared with cells transfected with the vector encoding the luciferase siRNA (control luc siRNA). 6-Phosphofructo-1-kinase, muscle isoform was used as protein loading control. (**e**) Treatment of GLUT3 (pEGFP.G3)- or GLUT1 (pEGFP.G1)-overexpressing HEK-293T cells with the vector encoding AMPK siRNA rendered cells unable to respond to NO by increasing the rate of GLUT3- or GLUT1-mediated glucose uptake. $^*P < 0.05$ versus control, $^\#P < 0.05$ versus pEGFP, †$P < 0.05$ versus pEGFP.G1.

vector encoding the siRNA against AMPK [28]. The efficacy of this approach was confirmed by Western blotting, which revealed a marked decrease in AMPK levels in comparison with control cells (Figure 3d) [24]. As shown in Figure 3(e), NO triggered a marked increase in glucose uptake after transfection with the control target sequence (luciferase siRNA-expressing pSuper) in cells overexpressing GLUT3 or, to a lesser degree, GLUT1. However, transfection with the AMPK-targeted siRNA rendered cells unable to respond to NO by increasing the rate of GLUT3- or GLUT1-mediated glucose uptake (Figure 3e).

DISCUSSION

In the present study, we have confirmed previous observations indicating that NO can stimulate the rate of glucose uptake [15–17]. However, those reports showed that the stimulatory effect of NO occurs through its ability to increase cGMP concentrations, whereas we show that GLUT3- and GLUT1-mediated glucose uptake was a cGMP-independent phenomenon. Furthermore, the cGMP-dependent pathway reported by others occurred in skeletal-muscle cells through a mechanism involving GLUT4 protein translocation [17]. In contrast, in the present study, we show that the activation of both GLUT3- and GLUT1-mediated glucose uptake by NO occurred in the absence of protein translocation. In addition, we show that the activation of GLUT3 transporter by NO was more sensitive than GLUT1, which was the main endogenous transporter expressed in the HEK-23T cells. Together, these results strongly suggest that the signalling cascade and physiological context leading to increased glucose uptake by NO would be different for GLUT3 and GLUT1 when compared with that for GLUT4.

To understand the mechanism(s) responsible for NO-activated GLUT3- and GLUT1-mediated glucose uptake, we focused on AMPK, a master regulator of cell energy metabolism in response to energetic stress [19]. In this sense, we have recently reported that both endogenous and exogenous NO switch on glycolysis through a mechanism involving AMPK [24]. Accordingly, we conjectured that the glucose catabolism induced by NO might be preceded by a concomitant availability of intracellular glucose. As judged by the increased AMPK-α_1-Thr-172 phosphorylation, NO would be activating AMPK, in strong agreement with our recent results found in astrocytes [24]. To check that AMPK mediates the increased glucose uptake initially triggered by NO, we transfected cells with a plasmid vector coding for the AMPK siRNA [24,28], leading the cells to contain much lower amounts of AMPK. Then, GLUT3- and GLUT1-overexpressing cells were exposed to NO, and we observed that AMPK disruption fully prevented the increases in glucose uptake by both transporters. These findings strongly suggest that the mechanism of this rapid up-regulation of GLUT3- and GLUT1-mediated glucose uptake by NO would be brought about through AMPK.

The above results are in apparent contradiction with those reported by Fryer et al. [17]. They suggest that the AMP-mimetic 5-aminoimidazole-4-carboxamide ribonucleoside stimulated AMPK in a manner resembling the increased AMP/ATP ratio that occurs during muscle contraction, leading skeletal-muscle cells to phosphorylate and activate eNOS [17,20]; the NO thus formed would then trigger cGMP-dependent GLUT4 translocation and activation [17]. In contrast, we propose that NO, formed by e.g. pro-inflammatory stimuli [8,25], can precede AMPK activation. In this sense, the inhibition of mitochondrial respiration by NO leads HEK-293T cells to increase the AMP/ATP ratio, a phenomenon compatible with the inhibition of cytochrome *c* oxidase by the free radical [25,32,37,38]. Consistent with the notion that AMPK is a cell energy sensor [19], the activation of AMPK by NO [24], the present study, would therefore represent a (patho)physiological cellular response to NO-dependent mitochondrial down-regulation. The possibility that GLUT3 and/or GLUT1 transporters simply play a permissive role in overall cell glucose consumption during NO activation of glycolysis cannot be disregarded [24]. However, others have shown that AMPK is capable of activating GLUT1 at the PM, i.e. without transporter translocation [22,23]. In view of the similarities that we found between GLUT1 and GLUT3 in the regulation by NO, it is tempting to suggest that NO-activated AMPK would promote a functional activation of the transporters at the PM.

GLUT3 is the main neuronal transporter, and it has been reported that cerebellar neurons show a high apparent affinity for glucose [2]. This observation has led to the suggestion that the expression of GLUT3 would be beneficial under ischaemic conditions [3–6], i.e. when the availability of the substrate as well as oxygen is low. In the present study, we show that the apoptotic death triggered by glucose deprivation was better prevented by GLUT3, when compared with GLUT1 overexpression. Moreover, glucose and oxygen deprivation are well-known factors that together induce NO formation, especially in the brain [12–14]. These results, together with our observation that the increase in

glucose uptake triggered by NO was higher in GLUT3-over-expressing cells, reinforce the notion that GLUT3 activity affords neuroprotection [39–42]. Furthermore, these findings are complementary to our recent results indicating that NO plays a cytoprotective role by switching on glycolysis through the cytochrome *c* oxidase–AMPK–6-phosphofructo-2-kinase pathway [24]. If so, the NO–cytochrome *c* oxidase–AMPK signalling cascade leading to GLUT3-mediated glucose uptake and glycolysis stimulation would represent a novel survival pathway during pathophysiological conditions involving transient reductions in the supply of cellular oxygen and glucose.

J. P. B. is funded by MCYT (SAF2001-1961/SAF2004-2038) and JCYL (SA081/04). A. P. is funded by FIS (03/1055) and JCYL (SA020/02). We thank Dr M. Delgado-Esteban, Ms Mónica Resch and Ms M. C. Alguerό for their excellent technical assistance, and Professor A. Zorzano for his critical reading of the manuscript.

REFERENCES

1 Maher, F., Vannucci, S. J. and Simpson, I. A. (1994) Glucose transporter proteins in brain. FASEB J. **8**, 1003–1011
2 Maher, F., Davies-Hill, T. M. and Simpson, I. A. (1996) Substrate specificity and kinetic parameters of GLUT3 in rat cerebellar granule neurons. Biochem. J. **315**, 827–831
3 Burant, C. F. and Bell, G. I. (1992) Mammalian facilitative glucose transporters: evidence for similar substrate recognition sites in functionally monomeric proteins. Biochemistry **31**, 10414–10420
4 Gerhart, D. Z., Broderius, M. A., Borson, N. D. and Drewes, L. R. (1992) Neurons and microvessels express the brain glucose transporter protein GLUT3. Proc. Natl. Acad. Sci. U.S.A. **89**, 733–737
5 Gould, G. W. and Seatter, M. J. (1997) Introduction to the facilitative glucose transporter family. In Facilitative Glucose Transporters (Gould, G. W., ed.), pp. 1–37, R.G. Landes Company, Austin, TX
6 Fattoretti, P., Bertoni-Freddari, C., Di Stefano, G., Casoli, T., Gracciotti, N., Solazzi, M. and Pompei, P. (2001) Quantitative immunohistochemistry of glucose transport protein (Glut3) expression in the rat hippocampus during aging. J. Histochem. Cytochem. **49**, 671–672
7 Hara, M., Matsuda, Y., Hirai, K., Okumura, N. and Nakagawa, H. (1989) Characteristics of glucose transport in neuronal cells and astrocytes from rat brain in primary culture. J. Neurochem. **52**, 902–908
8 Cidad, P., García-Nogales, P., Almeida, A. and Bolaños, J. P. (2001) Expression of glucose transporter GLUT3 by endotoxin in cultured rat astrocytes: the role of nitric oxide. J. Neurochem. **79**, 17–24
9 Maher, F. (1995) Immunolocalization of GLUT1 and GLUT3 glucose transporters in primary cultured neurons and glia. J. Neurosci. Res. **42**, 459–469
10 Galea, E., Feinstein, D. L. and Reis, D. J. (1992) Induction of calcium-independent nitric oxide synthase activity in primary rat glial cultures. Proc. Natl. Acad. Sci. U.S.A. **89**, 10945–10949
11 Simmons, M. L. and Murphy, S. (1992) Induction of nitric oxide synthase in glial cells. J. Neurochem. **59**, 897–905
12 Endoh, M., Maiese, K. and Wagner, J. (1994) Expression of the inducible form of nitric oxide synthase by reactive astrocytes after transient global ischemia. Brain Res. **651**, 92–100
13 Moro, M. A., DeAlba, J., Leza, J. C., Lorenzo, P., Fernandez, A. P., Bentura, M. L., Bosca, L., Rodrigo, J. and Lizasoain, I. (1998) Neuronal expression of inducible nitric oxide synthase after oxygen and glucose deprivation in rat forebrain slices. Eur. J. Neurosci. **10**, 445–456
14 Iadecola, C. (1997) Bright and dark sides of nitric oxide in ischemic brain injury. Trends Neurosci. **20**, 132–139
15 Etgen, Jr, G. J., Fryburg, D. A. and Gibbs, E. M. (1997) Nitric oxide stimulates skeletal muscle glucose transport through a calcium/contraction- and phosphatidylinositol-3-kinase-independent pathway. Diabetes **46**, 1915–1919
16 Roberts, C. K., Barnard, R. J., Scheck, S. H. and Balon, T. W. (1997) Exercise-stimulated glucose transport in skeletal muscle is nitric oxide dependent. Am. J. Physiol. **273**, E220–E225
17 Fryer, L. G., Hajduch, E., Rencurel, F., Salt, I. P., Hundal, H. S., Hardie, D. G. and Carling, D. (2000) Activation of glucose transport by AMP-activated protein kinase via stimulation of nitric oxide synthase. Diabetes **49**, 1978–1985
18 Hardie, D. G., Carling, D. and Sim, A. T. R. (1989) The AMP-activated protein kinase: a multisubstrate regulator of lipid metabolism. Trends Biochem. Sci. **14**, 20–23
19 Carling, D. (2004) The AMP-activated protein kinase cascade – a unifying system for energy control. Trends Biochem. Sci. **29**, 18–24
20 Chen, Z. P., Mitchelhill, K. I., Michell, B. J., Stapleton, D., Rodriguez-Crespo, I., Witters, L. A., Power, D. A., Ortiz de Montellano, P. R. and Kemp, B. E. (1999) AMP-activated protein kinase phosphorylation of endothelial NO synthase. FEBS Lett. **443**, 285–289
21 Shi, Y., Liu, H., Vanderburg, G., Samuel, S. J., Ismail-Beigi, F. and Jung, C. Y. (1995) Modulation of GLUT1 intrinsic activity in clone 9 cells by inhibition of oxidative phosphorylation. J. Biol. Chem. **270**, 21772–21778
22 Abbud, W., Habinowski, S., Zhang, J. Z., Kendrew, J., Elkairi, F. S., Kemp, B. E., Witters, L. A. and Ismail-Beigi, F. (2000) Stimulation of AMP-activated protein kinase (AMPK) is associated with enhancement of Glut1-mediated glucose transport. Arch. Biochem. Biophys. **380**, 347–352
23 Barnes, K., Ingram, J. C., Porras, O. H., Barros, L. F., Hudson, E. R., Fryer, L. G., Foufelle, F., Carling, D., Hardie, D. G. and Baldwin, S. A. (2002) Activation of GLUT1 by metabolic and osmotic stress: potential involvement of AMP-activated protein kinase (AMPK). J. Cell Sci. **115**, 2433–2442
24 Almeida, A., Moncada, S. and Bolaños, J. P. (2004) Nitric oxide switches on glycolysis through the AMP protein kinase and 6-phosphofructo-2-kinase pathway. Nat. Cell Biol. **6**, 45–51
25 Bolaños, J. P., Peuchen, S., Heales, S. J. R., Land, J. M. and Clark, J. B. (1994) Nitric oxide-mediated inhibition of the mitochondrial respiratory chain in cultured astrocytes. J. Neurochem. **63**, 910–916
26 Almeida, A., Almeida, J., Bolaños, J. P. and Moncada, S. (2001) Different responses of astrocytes and neurons to nitric oxide: the role of glycolytically-generated ATP in astrocyte protection. Proc. Natl. Acad. Sci. U.S.A. **98**, 15294–15299
27 Burkhalter, J., Fiumelli, H., Allaman, I., Chatton, J. Y. and Martin, J. L. (2003) Brain-derived neurotrophic factor stimulates energy metabolism in developing cortical neurons. J. Neurosci. **23**, 8212–8220
28 Brummelkamp, T. R., Bernards, R. and Agami, R. (2002) A system for stable expression of short interfering RNAs in mammalian cells. Science **296**, 550–553
29 Sledz, C. A., Holko, M., de Veer, M. J., Silverman, R. H. and Williams, R. G. (2003) Activation of the interferon system by short-interfering RNAs. Nat. Cell Biol. **9**, 834–839
30 Ohtsuka, T., Ryu, H., Minamishima, Y. A., Macip, S., Sagara, J., Nakayama, K. I., Aaronson, S. A. and Lee, S. W. (2004) ASC is a Bax adaptor and regulates the p53-Bax mitochondrial apoptosis pathway. Nat. Cell Biol. **6**, 121–128
31 Hobbs, A. J. and Moncada, S. (2003) Antiplatelet properties of a novel, non-NO-based soluble guanylate cyclase activator, BAY 41-2272. Vasc. Pharmacol. **40**, 149–154
32 Brown, G. C. and Cooper, C. E. (1994) Nanomolar concentrations of nitric oxide reversibly inhibit synaptosomal respiration by competing with oxygen at cytochrome oxidase. FEBS Lett. **356**, 295–298
33 Jaworek, D. and Weisch, J. (1985) Adenosine 5′-diphosphate and adenosine 5′-monophosphate. UV-method. In Methods of Enzymatic Analysis, vol. VII (Bergmeyer, J. and Graßl, M., eds.), pp. 365–370, Verlag Chemie, Weinheim, Deerfield Beach (FL), Basel
34 Lowry, O. H., Rosebrough, N. J., Lewis-Farr, A. and Randall, R. J. (1951) Protein measurement with the Folin phenol reagent. J. Biol. Chem. **193**, 265–275
35 Suarez, E., Bach, D., Cadefau, J., Palacin, M., Zorzano, A. and Guma, A. (2001) A novel role of neuregulin in skeletal muscle. Neuregulin stimulates glucose uptake, glucose transporter translocation, and transporter expression in muscle cells. J. Biol. Chem. **276**, 18257–18264
36 Bradford, M. M. (1976) A rapid and sensitive method for the quantitation of microgram quantities of protein utilizing the principle of protein-dye binding. Anal. Biochem. **72**, 248–254
37 Cleeter, M. W. J., Cooper, J. M., Darley-Usmar, V. M., Moncada, S. and Schapira, A. H. (1994) Reversible inhibition of cytochrome c oxidase, the terminal enzyme of the mitochondrial respiratory chain, by nitric oxide. Implications for neurodegenerative diseases. FEBS Lett. **345**, 50–54
38 Schweizer, M. and Richter, C. (1994) Nitric oxide potently and reversibly deenergizes mitochondria at low oxygen tension. Biochem. Biophys. Res. Commun. **204**, 169–175
39 Hara, M., Matsuda, Y., Hirai, K., Okumura, N. and Nakagawa, H. (1989) Effect of glucose starvation on glucose transport in neuronal cells in primary culture from rat brain. J. Neurochem. **52**, 909–912
40 Lee, W. H. and Bondy, C. A. (1993) Ischemic injury induces brain glucose transporter gene expression. Endocrinology **133**, 2540–2544
41 Urabe, T., Hattori, N., Nagalatsu, S., Sawa, H. and Mizuno, Y. (1996) Expression of glucose transporters in rat brain following transient focal ischemic injury. J. Neurochem. **67**, 265–271
42 Uehara, Y., Nipper, V. and McCall, A. L. (1997) Chronic insulin hypoglycemia induces GLUT-3 protein in rat brain neurons. Am. J. Physiol. **272**, E716–E719

Received 26 May 2004/3 August 2004; accepted 23 August 2004
Published as BJ Immediate Publication 23 August 2004, DOI 10.1042/BJ20040886